

TECHNICAL NOTE

Andrew G. Tallin¹ and Carlos Santamarina¹

Geotomography in Site Investigation: Simulation Study

REFERENCE: Tallin, A. G. and Santamarina, J. C., "Geotomography in Site Investigation: Simulation Study," *Geotechnical Testing Journal*, GTJODJ, Vol. 13, No. 2, June 1990, pp. 129-133.

ABSTRACT: Tomography is the reconstruction of images from measurements of line integrals. It is used in a variety of scientific and technical applications. Advances in electronics and computers make the technique accessible to geotechnical engineering. The combination of penetration testing and tomographic reconstruction would result in a powerful site investigation tool.

A tomographic software was developed in this research. This paper discusses the fundamentals of the procedure and presents the results of a simulation study using the algebraic reconstruction technique (ART). The parametric study involves field set-up conditions, number of instruments per side, and the size of the grid used in the reconstruction.

KEY WORDS: tomography, site investigation, penetration tests, cross-hole testing

Tomography is a widely used technique in medical diagnosis and in other areas including geophysics. Advances in the power and precision of modern electronic equipment and computers, along with the reduction in cost, make the technique accessible to other applications. This paper deals with the use of geotomography in geotechnical engineering. Recent developments in site investigation provide the field tools that are needed for its implementation; for example, down-hole [1-2] and cross-hole measurements [3] using the seismic cone (SCPT) may be processed by tomographic techniques.

Geotomography can be based either on electromagnetic or mechanical waves. The development of electromagnetic geophysical tomography started in the mid-seventies at Lawrence Livermore Laboratory [4] as an adaptation of computerized axial tomography (CAT), which had been successfully used in medical diagnosis. However, standard transformation techniques used in axial tomography require that the reconstruction area be circular with 360° of data. This is impractical for geotechnical applications, which are characterized by trapezoidal cross sections and primarily by an incomplete angular coverage.

Geophysical tomography based on mechanical waves advances the processing of standard cross-hole data, allowing a systematic and global evaluation of the measurements [5-6]. Geophysical

seismic tomography has been used to study rectangular regions greater than 100 m on a side [7]. Sources have included airguns, explosives, and earthquake data. These tools were developed for mineral and petroleum exploration and for the study of radioactive disposal sites.

Tomographic Reconstruction

Tomographic reconstruction operates on a large set of measurements which are line integrals of the form [8]

$$y_i = \int_a^b x[g_i(s)] ds \quad (1)$$

where the vector function $g_i(s)$ is the equation of the arc from the source a to the receiver b , and the function $x(z)$ is the value of the image at location z , called the picture function. In mechanical wave based geotomography, the picture function $x(z)$ is the inverse of the elastic wave velocity, the *slowness*. The measurement y_i is the total transit time of the wave from the source a to the sensor b . In electromagnetic geotomography the measurement y_i is the attenuation, and the picture function $x(z)$ is the absorption rate at z .

The image is discretized into a plane of rectangular cells or pixels, with values $x = (x_1 \dots x_N)$. If $y = (y_1 \dots y_M)$ is the vector of all the measurements, the relationship between all the cell values and the measurements is

$$y = Rx \quad (2)$$

where the M by N matrix R has elements r_{ij} , which represent the transit length of the j th cell by the i th arc. The total transit length in the j th cell is the sum of r_{ij} for all arcs i .

In practice, the number of measurements significantly exceeds the number of the pixels in most cases. The goal of reconstruction is to minimize the difference between the measurements and the estimate of the measurements calculated from the pixel map, x . For example, if the measurement of error is the squared error, then the reconstruction problem becomes the least squares problem

$$x \ni [y - Rx]^T [y - Rx] \text{ is a minimum} \quad (3)$$

¹Assistant professor, Polytechnic University, 333 Jay St., Brooklyn, NY 11201.

This can be solved directly by carryout out the inner product and differentiating with respect to x , resulting in the solution

$$x = [R'R]^{-1}R'y \quad (4)$$

The amount of information available to determine a cell value is related to the total transit length of the rays crossing the cell. In addition to the total transit length, the similarity between the paths crossing a given cell is also important. For example, if a source-sensor pair was used many times at the same position, one could make more measurements than the number of cells; however, the data would not allow for the reconstruction of the variable field conditions between the source and the sensor. In this case every row in $R'R$ is the same.

This observation can be generalized to real situations. If a large number of paths are nearly parallel, the matrix $R'R$ is singular or ill-conditioned, and reconstruction becomes impossible.

Direct solution of Eq 4 would require the solution of N simultaneous linear equations. For realistic cases, R is large and sparse and in general has no distinct structure, such as the banded structure of matrices in structural analysis. In such cases, storage, formation, and solution of $R'R$ are impractical. Consequently, reconstruction of nonaxial images is done by applying an iterative solution, using the following operation defined for each measurement i

$$x^{(1)} = P_i x^{(0)} = x^{(0)} + \lambda r_i [y_i - r'_i x^{(0)}] / r'_i r_i \quad (5)$$

where λ is an acceleration constant between 0 and 2, and $x^{(0)}$ and $x^{(1)}$ are the initial and updated pictures. In the algebraic reconstruction technique (ART), the operator P_i is used recursively to update x after each datum is used.

$$\hat{x} = P_{M-1} P_{M-2} \dots P_0 x^{(0)} \quad (6)$$

On the other hand, the simultaneous image reconstruction technique (SIRT) uses the operator on all the data before updating the pixel map

$$\hat{x} = 1/M \sum_{i=0}^{M-1} P_i x^{(0)} \quad (7)$$

The estimate of the picture \hat{x} is simply the average of each of the pictures that results from updating the image on the basis of each datum y_i .

In both methods, the picture estimated in a given cycle \hat{x} is the initial picture $x^{(0)}$ for the next updating cycle. This is repeated until the change in the estimated picture function is small.

The matrix R is relatively easy to construct for linear ray paths, *i.e.* arcs g_i are straight lines. The problem becomes much more difficult if ray bending due to refraction is to be accounted for. One alternative is to start reconstruction by assuming that the ray paths are straight. Then the matrix R is modified by ray tracing to account for the refraction which would be present in this initial image. Using the new matrix R the image is reconstructed. This procedure is repeated several times until a stable image is found.

Data based on electromagnetic waves indicate that the straight ray reconstruction leads to marginal results when variations in wave velocity exceed about 30% [9]. Still, much research is taking

place to include ray bending in the reconstruction algorithms for geophysical applications [10].

Parametric Study

A computer program was written to perform ART on rectangular regions. A second program was written to artificially generate field data (travel times), given a soil stratigraphy and the location of sensors and sources. Both are based on the assumption of linear ray paths.

The reconstruction program takes the artificially generated data and the geometry of the problem as input. Intersection points for each of the cell boundaries are determined, and the length of the line segment in the j^{th} cell for the i^{th} arc is the value of the r_{ij} element of R . The image is continuously displayed after each iteration. Depending on the number of pixels and the number of rays, the rate of image updating ranges from 30 times per minute for a coarse grid of 8 by 8 and 256 rays, to three updatings per minute for a grid of 32 by 32 and 4096 rays, when an engineering workstation is used (Sun 3/60).

Different stratigraphies have been selected to study the quality of the reconstructed image. Cross sections are assumed square, L by L . In each case, the reconstructed image is evaluated taking into consideration the transit lengths in the pixels. This allows the assessment of the resolution and the reliability of the image pixels. No image enhancement has been used in the figures shown in this publication.

Instrumented Sides

The effect of different field arrangements was studied: (a) full setup, with emission and reception in two boreholes and reception on the surface; (b) partial setup, with emission from one borehole and reception at the other borehole and at the surface; and (c) standard cross-hole arrangement with emission from one borehole and reception in the other. In the three cases, 32 sources or receivers were placed on the instrumented sides, and reconstruction was performed for a 32 by 32 grid.

The stratigraphy that was selected was composed of two layers with interface along the diagonal. Figure 1 shows the reconstructed images after 100 iterations and the total transit length per pixel in each case. The stratigraphy is clearly defined in the three images, even though the amount of information from cross-hole measurements is much more limited than from the other two arrangements. The same observation was made for other simple field conditions, including horizontal stratification.

The transit length plots show the variability in the quality of the reconstruction. The full set-up results in good reconstruction everywhere except for the region below 0.8 L . In the second case, with emission from only one borehole, reconstruction is better in the triangle bounded by the two sides with sensors. The quality of the image obtained from the cross-hole setup is no better at the surface than it is at the bottom edge; in this case, the ability to resolve borehole-to-borehole discontinuous structures is best in the region near the middle of the image where the transit length density is high.

Resolution in the Reconstruction

The reconstruction can be performed to any level of resolution, but the use of very small pixels may result in cells with no transit

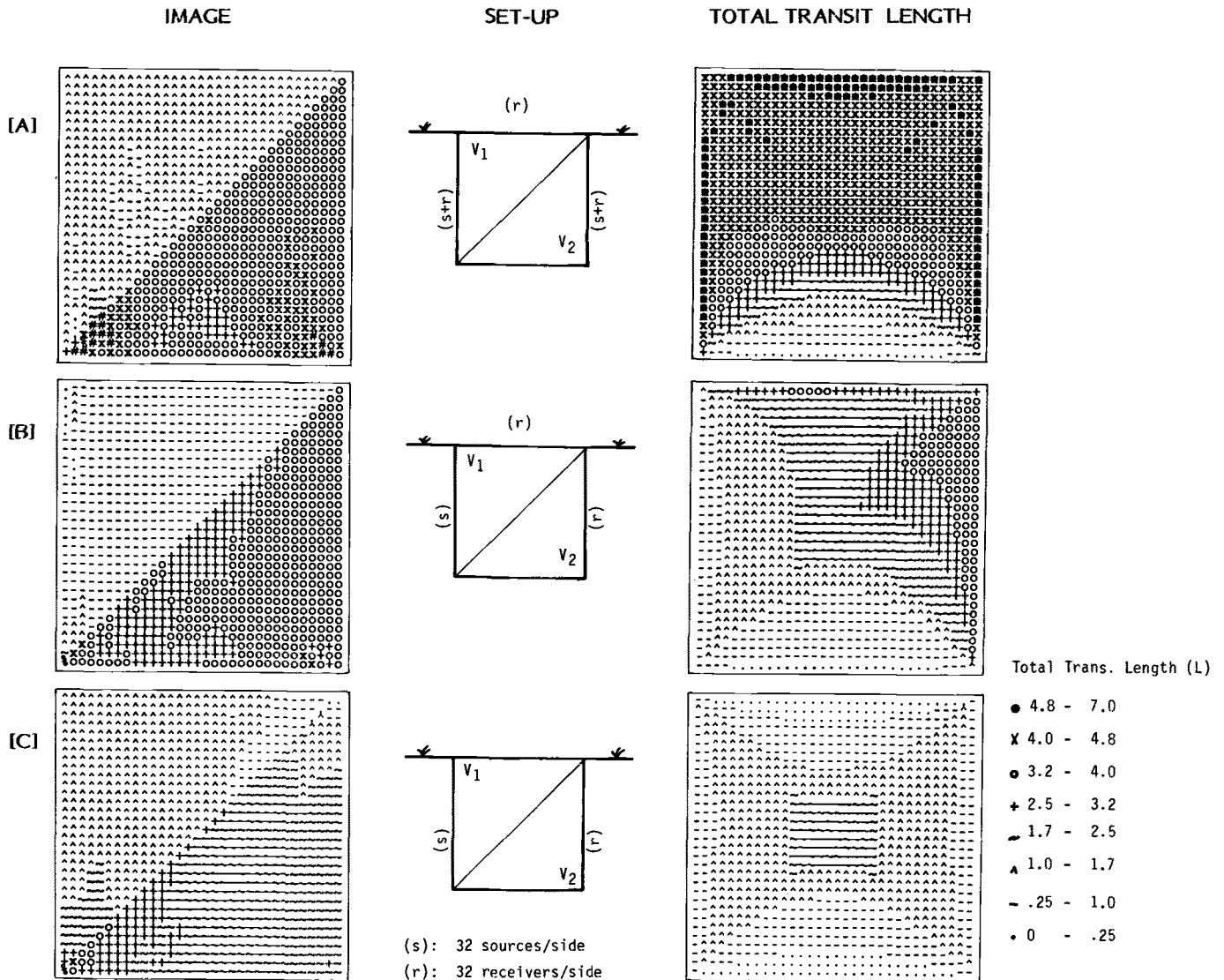


FIG. 1—Effect of different field setup (100 iterations).

length. In this case, $R'R$ has entire rows and columns equal to 0, and direct solution for x using Eq 4 is not possible. However, ART is not mathematically affected by the singularity of $R'R$ because the operation P_i (Eq 5) only updates the picture function $x(z)$ for cells with nonzero transit length. Nevertheless, if the matrix $R'R$ is ill conditioned, the solution does not converge to an exact solution.

Still, the selection of the cell size is a relevant input parameter. A stratigraphy consisting of an inclusion in a homogeneous medium was used to demonstrate this effect. Sources and receivers were placed in a full setup on the lateral sides and on the surface, simulating 16 instruments per side. Reconstruction was done for 32 by 32, 16 by 16 and 8 by 8 grids. The reconstructed images and the transit lengths in each case are shown in Fig. 2. The comparison of Figures 2A and 2B shows the blurring effect of enforcing higher resolution, due to the reduced transit length in the cells of images with small pixels. On the other hand, increasing the size of the pixel beyond the discretization used for the

instrumentation increases the granularity without a major improvement of the image. The selection of the optimal number of cells is not simple; discretizing sides to match the instrumentation appears to be a good choice.

Image-enhancing techniques can be used to smooth or contrast the image. This involves an assumption about the in-situ conditions; however, in most cases, no new measured data are incorporated. *A priori* knowledge of the geological formation processes can be used for the selection of smoothing matrices. For example, one could select a filter that increases the contrast of horizontal lines if a layered stratigraphy is under investigation.

Number of Instruments

The size of detectable stratigraphic details depends on the number of the instruments used, the spacing, and the location. In order to demonstrate the effects of the amount of instrumentation, a complex stratigraphy was chosen composed of four soil

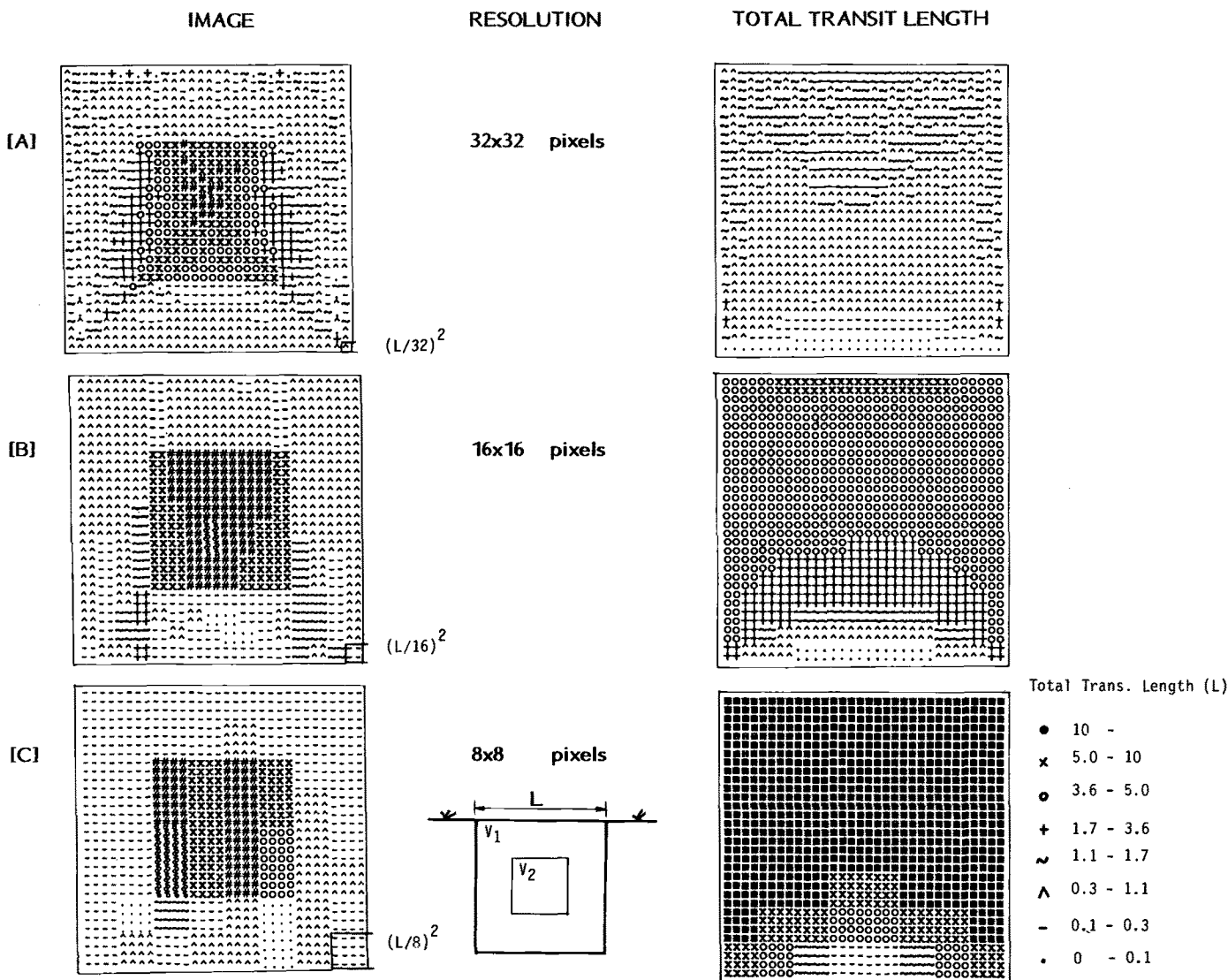


FIG. 2—Resolution in the reconstructed image (100 iterations).

layers with inclined boundaries. The full setup configuration was used, with sources on two sides and receivers on three sides. Three levels of instrumentation with 32, 16, and 8 sources/sensors per side were simulated. Based on the previous results, reconstruction was done on cell grids corresponding to the instrumentation levels, 32 by 32, 16 by 16, and 8 by 8. The images (Fig. 3) indicate that reconstructions are very good and show the character of the stratigraphy in all three cases. However, the level of detail is quite different ranging from $L/32$ to $L/8$. The reduced amount of information in the lower part of the cross section (see Fig. 1A) manifests in the blurring of the image in this region for all levels of instrumentation.

Other Observations

In addition to the results presented here, other studies were performed. In general, it was found that inclusions can be easily depicted, that reconstruction is very sensitive to the number of

instrumented sides for a given layering condition, and that reconstruction of cross-hole data gave good results for the common case of horizontal layering. However, cross-hole data proved insufficient for more complex profiles such as the one in Fig. 3.

Reconstruction based on the SIRT algorithm was also programmed. At least for the images that were investigated, ART performed better than SIRT. However, convergence may be improved with SIRT [11].

Final Comments

Tomographic reconstruction is a powerful technique. It is relatively easy to implement, at least for the assumption of linear ray paths. Because of innovations in electronics, the field equipment needed can be developed at reasonable cost. The recent advances in penetration testing point towards the development of geotomography based on seismic cone penetration test SCPT data. The result would be a powerful tool that would combine

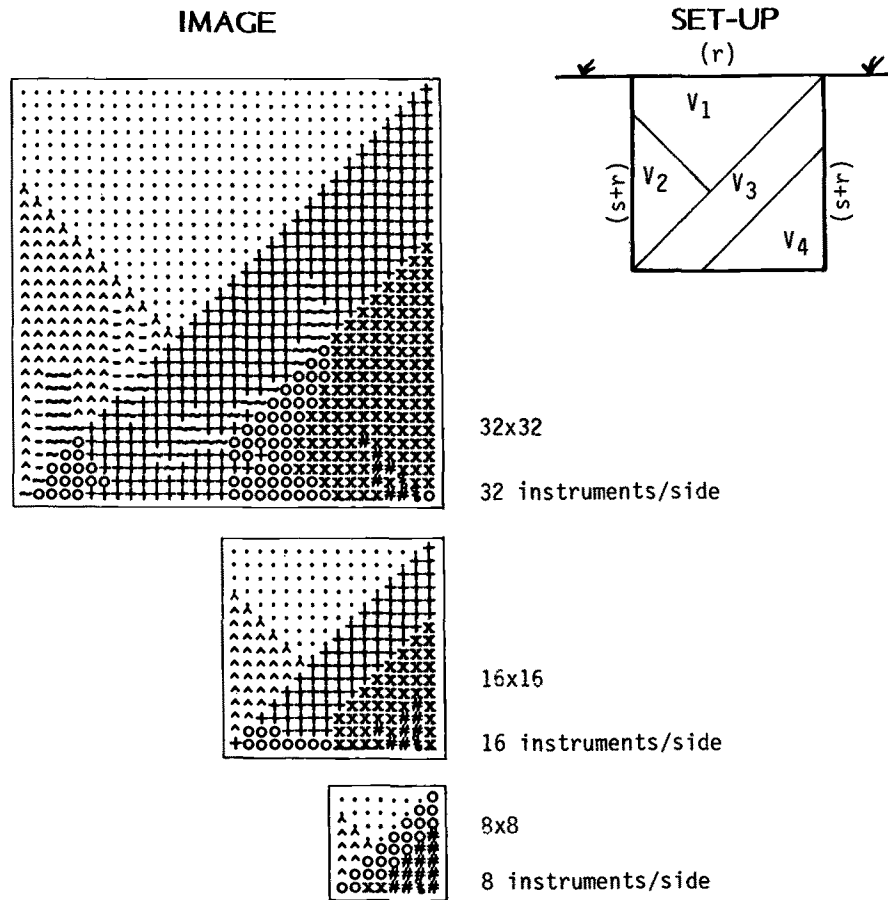


FIG. 3—Effect of number of instruments (100 iterations).

the extensive geotechnical experience in penetration testing with imaging techniques, allowing for the visualization of underground conditions.

References

- [1] Campanella, R. G., Robertson, P. K., and Gillespie, D., "Seismic Cone Penetration Test," *Use of In Situ Tests in Geotechnical Engineering*, ASCE, New York, 1986, pp. 116–130.
- [2] Robertson, P. K., Campanella, R. G., Gillespie, D., and Rice, A., "Seismic SPT to Measure In-Situ Shear Wave Velocity," *ASCE Journal of Geotechnical Division*, Vol. 112, No. 8, 1986, pp. 791–803.
- [3] Baldi, G., Bruzzi, D., Superbo, S., Battaglio, M., and Jamiolkowski, M., "Seismic Cone in Po River Sand," *Penetration Testing—ISOPT 1*, Balkema, Ed. De Ruyter, 1988, Florida, pp. 643–649.
- [4] Lytle, R. J., "Geophysical Characterization Using Advanced Data Processing," Proceedings, ASCE Conference on Site Characterization and Exploration, ASCE, New York, 1978, pp. 291–301.
- [5] Ivansson, S., "Seismic Borehole Tomography—Theory and Computational Methods," *Proceedings of the IEEE*, IEEE, New York, Vol. 74, No. 2, 1986, pp. 328–338.
- [6] Ivansson, S., "A Study of Methods for Tomographic Velocity Estimation in the Presence of Low Velocity Zones," *Geophysics*, Vol. 50, No. 6, 1985, pp. 969–988.
- [7] Mutter, J. C., "Seismic Images of Plate Boundaries," *Scientific American*, Vol. 251, February 1984, pp. 66–68.
- [8] Herman, G. T., *Image Reconstruction from Projections; The Fundamentals of Computerized Tomography*, Academic Press, San Francisco, 1980.
- [9] Witten, A. J. and Long, E., "Shallow Applications of Geophysical Diffraction Tomography," *IEEE Transactions on Geoscience and Remote Sensing*, Vol. GE-24, No. 5, IEEE, New York, 1986, pp. 654–662.
- [10] Lytle, R. F. and Dines, K. A., "Iterative Ray Tracing Between Boreholes for Underground Image Reconstruction," *IEEE Transactions on Geoscience and Remote Sensing*, Vol. GE-18, No. 3, IEEE, New York, pp. 234–240.
- [11] Dines, K. A. and Lytle, R. F., "Computerized Geophysical Tomography," *Proceedings of the IEEE*, Vol. 67, No. 7, IEEE, New York, 1979, pp. 1065–1073.